EUKARYOTIC CELL, Feb. 2006, p. 411–421 Vol. 5, No. 2
1535-9778/06/$08.00+0 doi:10.1128/EC.5.2.411–421.2006

Vacuolar Membrane Dynamics in the Filamentous Fungus *Aspergillus oryzae*†

Jun-ya Shoji, Manabu Arioka, and Katsuhiko Kitamoto*

Department of Biotechnology, The University of Tokyo, 1-1-1 Yayoi, Bunkyo-ku, Tokyo 113-8657, Japan

Received 16 August 2005/Accepted 18 October 2005

Vacuoles in filamentous fungi are highly pleomorphic and some of them, e.g., tubular vacuoles, are implicated in intra- and intercellular transport. In this report, we isolated Ao*vam3*, the homologue of the *Saccharomyces cerevisiae VAM3* gene that encodes the vacuolar syntaxin, from *Aspergillus oryzae*. In yeast complementation analyses, the expression of Ao*vam3* restored the phenotypes of both Δ*vam3* and Δ*pep12* mutants, suggesting that AoVam3p is likely the vacuolar and/or endosomal syntaxin in *A. oryzae*. FM4-64 [*N*-(3-triethylammoniumpropyl)-4-(*p*-diethylaminophenyl-hexatrienyl)pyridinium dibromide] and CMAC (7-amino-4-chloromethylcoumarin) staining confirmed that the fusion protein of enhanced green fluorescent protein (EGFP) with AoVam3p (EGFP-AoVam3p) localized on the membrane of the pleomorphic vacuolar networks, including large spherical vacuoles, tubular vacuoles, and putative late endosomes/prevacuolar compartments. EGFP-AoVam3p-expressing strains allowed us to observe the dynamics of vacuoles with high resolutions, and moreover, led to the discovery of several new aspects of fungal vacuoles, which have not been discovered so far with conventional staining methods, during different developmental stages. In old hyphae, EGFP fluorescence was present in the entire lumen of large vacuoles, which occupied most of the cell, indicating that degradation of cytosolic materials had occurred in such hyphae via an autophagic process. In hyphae that were not in contact with nutrients, such as aerial hyphae and hyphae that grew on a glass surface, vacuoles were composed of small punctate structures and tubular elements that often formed reticulum-like networks. These observations imply the presence of so-far-unrecognized roles of vacuoles in the development of filamentous fungi.

Vacuoles are acidic compartments that are important for metabolite storage and cytosolic ion and pH homeostasis (for a review, see reference 18). In the unicellular yeast *Saccharomyces cerevisiae*, roles of and transport pathways to vacuoles have been extensively studied. Especially, many studies have been focused on the syntaxin family t-SNAREs (target organelle soluble *N*-ethyl-maleimide-sensitive factor [NSF] attachment protein receptors), which are central molecules of intracellular vesicular transport. t-SNAREs that reside on the target organelle membrane mediate the fusion of transport vesicles with the organelles via the specific interaction with vesicle SNAREs on the transport vesicles (29). *S. cerevisiae* Pep12p is the syntaxin family t-SNARE on the late endosome/prevacuolar compartment and receives Golgi-derived vesicles (3). Vam3p is the vacuolar membrane syntaxin that regulates the vesicular traffic to and the homotypic fusion of vacuoles (44). Since *S. cerevisiae* Vam3p localizes exclusively on the vacuolar membrane, Vam3p is frequently used for visualization of vacuoles (45, 46) and as a marker of vacuoles in subcellular fractionation experiments. AtVam3p is a Vam3p-homologue protein in *Arabidopsis thaliana* (30), and its fusion protein with green fluorescent protein (GFP) has been successfully used for the observation of vacuolar dynamics in *A. thaliana* (41) and *Nicotiana tabacum* (22).

On the other hand, characteristic aspects of the vacuoles in multicellular fungi were eventually identified using microscopic approaches in the past decade. First, vacuoles in filamentous fungi display approximately predictable pleomorphism in the different regions of the mycelia; vacuoles are typically rare or absent in the apical region, whereas ovoid-spherical vacuoles are present in the subapical region, tubular vacuoles in the more distal region, and large spherical vacuoles in the basal zone (14). Second is the presence of highly motile tubular vacuoles that can be visualized by vacuolar fluorescent probes such as 6-carboxyfluorescein diacetate (CFDA) derivatives (2, 6, 7, 34, 42) or *N*-(3-triethylammoniumpropyl)-4-(*p*-diethylaminophenyl-hexatrienyl)pyridinium dibromide (FM4-64) (10) and by the fusion protein of carboxypeptidase Y (CPY) with enhanced GFP (EGFP) (23, 24). These characteristic vacuolar morphologies indicate that the vacuoles may have particular roles in filamentous fungi. In fact, the tubular vacuoles that were originally found in a mycorrhizal fungus *Pisolithus tinctorius* (34) were implicated in intra- and intercellular transport of nutrients (reviewed in reference 2). In spite of these intriguing observations, however, molecular genetics studies on vacuoles in filamentous fungi have been limited (25, 26, 39). Therefore, identification and investigation of the proteins involved in vacuolar morphogenesis are now crucial for further understanding of the molecular mechanisms regulating pleomorphic vacuoles in filamentous fungi.

In this report, we developed *Aspergillus oryzae* strains that express the fusion protein of EGFP with AoVam3p, the Vam3p homologue in *A. oryzae*. As EGFP-AoVam3p localized on the vacuolar membrane, these strains enabled us to observe vacuolar membrane dynamics in *A. oryzae* with high resolution.

* Corresponding author. Mailing address: Department of Biotechnology, The University of Tokyo, 1-1-1 Yayoi, Bunkyo-ku, Tokyo 113-8657, Japan. Phone: 81 3 5841 5161. Fax: 81 3 5841 8033. E-mail: akitamo@mail.ecc.u-tokyo.ac.jp.

† Supplemental material for this article may be found at http://ec.asm.org/.

MATERIALS AND METHODS

Plasmids and strains. Primer pairs vam3 Bsr-N (5′-CTGTACATGTATTTC GACCGTCTTAGT-3′) and vam3 Bsr-C (5′-TGTACATTATCCAATAGTAG CCGCCAG-3′) were designed (BsrGI sites are underlined) based on the expressed sequence tag sequence of a putative *VAM3* homologue gene in *A. oryzae* (Ao*vam3*). The Ao*vam3* cDNA (0.8 kb) was amplified with these primer pairs, using the *A. oryzae* RIB40 cDNA library as a template. The *egfp* gene (0.7 kb) was fused to the 5′ end of the resultant Ao*vam3* cDNA in frame, resulting in an *egfp*-Ao*vam3* cDNA fusion gene. Two plasmids for the expression of the fusion gene were subsequently constructed. The plasmid pUEGFP-VAM carries the 0.6-kb *amyB* promoter, followed by the 1.5-kb *egfp*-Ao*vam3* fusion gene, the 0.3-kb *nos3′* terminator, and the 5.5-kb *niaD* gene encoding a nitrate reductase as a transformation marker. This plasmid was introduced to *A. oryzae* niaD300 (*niaD*$^-$) strain with the *A. oryzae* transformation procedure (17), yielding UEV strains. The plasmid pBNVPEV carries the 1.3-kb Ao*vam3* promoter followed by the 1.5-kb *egfp*-Ao*vam3* fusion gene, the 0.3-kb *nos3′* terminator, and the 5.5-kb *niaD* marker. For the generation of Ao*vam3* conditional expression strains, TPVIIs, a DNA fragment that contained Ao*vam3* 5′ flanking region followed by *Aspergillus nidulans sC* marker encoding an ATP sulfurylase, *A. oryzae thiA* promoter driving Ao*vam3* cDNA, and Ao*vam3* 3′ flanking region, was introduced into *A. oryzae* NS4 strain (*niaD*$^-$, *sC*$^-$). The gene replacement of Ao*vam3* by *thiA* promoter-driven Ao*vam3* cDNA was confirmed by PCR and Southern analysis (data not shown). The plasmid pBNVPEV was introduced to one of the conditional expression strains, the TPVII118 strain, yielding TPVEV strains. Southern analysis of the genomic DNA of TPVEV1, 2, 3, and 4 revealed that single copies of the plasmid had been inserted homologously at the *niaD* locus in the TPVEV1, 2, and 3 strains, while a few extra copies of the plasmid (probably one or two additional copies, judged by the signal intensity) had been inserted in the TPVEV4 strain (data not shown).

For yeast complementation analyses, deletion strains of EUROSCARF (http://www.rz.uni-frankfurt.de) constructed from *S. cerevisiae* BY4741 (*MAT***a** *his3Δ1 leu2Δ0 met5Δ0 ura3Δ0*) (5) were used. Ao*vam3* cDNA was amplified using the Vam3 N-term (5′-CATGTATTTCGACCGTCTTAG-3′) and Vam3 C-term (5′-TTATCCAATAGTAGCCGCCAG-3′) primers and subsequently inserted downstream of the *GAL1* promoter of the pYES2 plasmid. The obtained plasmid, pYESVAM, was introduced into the yeast Δ*vam3* strain Y02362 (BY4741 *vam3*Δ::*KanMX4*) and Δ*pep12* strain Y01812 (BY4741 *pep12*Δ::*KanMX4*). pYES2 alone was also introduced into the Δ*vam3* and Δ*pep12* strains to obtain the control strains.

Culture conditions. Czapek-Dox medium (CD; 0.3% $NaNO_3$, 0.2% KCl, 0.1% KH_2PO_4, 0.05% $MgSO_4 \cdot 7H_2O$, 0.002% $FeSO_4 \cdot 7H_2O$, 2% glucose, pH 5.5) was used for microscopic observations. M medium [0.2% NH_4Cl, 0.1% $(NH_4)_2SO_4$, 0.05% KCl, 0.05% NaCl, 0.1% KH_2PO_4, 0.05% $MgSO_4 \cdot 7H_2O$, 0.002% $FeSO_4 \cdot 7H_2O$, 2% glucose, pH 5.5] was used for comparison of phenotypes between TPVII118 and TPVEV strains. Thiamine hydrochloride (Sigma Chemical Co., St. Louis, MO) was added for observation of TPVEV strains at a concentration of 10 μM. DPY (2% dextrin, 1% polypeptone, 0.5% yeast extract, 0.5% KH_2PO_4, 0.05% $MgSO_4 \cdot 7H_2O$) was used for observation of vacuoles in germinating conidia.

A YPGal plate (1% yeast extract, 2% Bacto-peptone, and 2% galactose) was used to compare the growth of yeast strains. For the CFDA staining of yeast vacuoles, SGal medium (0.67% yeast nitrogen base without amino acids, 2% galactose, with required nutrients) was used.

Microscopic equipment. For routine microscopy we used an Olympus System microscope model BX52 (Olympus, Tokyo, Japan) equipped with a UPlanApo 100× objective lens (1.35 numerical aperture) (Olympus). A GFP filter (495/20 nm excitation, 510 nm dichroic, 530/35 nm emission) (Chroma Technologies, Brattleboro, VT) or a U-MWIB filter cube (460 to 490 nm excitation, 505 nm dichroic, >515 nm emission) (Olympus) was used for observation of EGFP fluorescence. A DsRed filter (570/20 nm excitation, 590 nm dichroic, 630/60 nm emission) (Chroma Technologies) and a BH-DMU (330 to 385 nm excitation, 400 nm dichroic, >420 nm emission) UV excitation cube (Olympus) were used to observe the fluorescence of *N*-(3-triethylammoniumpropyl)-4-(*p*-diethylaminophenyl-hexatrienyl)pyridinium dibromide (FM4-64) (Molecular Probes Inc., Eugene, OR) and 7-amino-4-chloromethylcoumarin (CMAC) (Molecular Probes Inc.), respectively. Images were analyzed with MetaMorph software (Molecular Devices Co., Sunnyvale, CA).

Confocal microscopy was performed with an IX70 inverted microscope (Olympus) equipped with 100× and 40× Neofluor objective lenses (1.30 numerical aperture), a Sapphire 488-20, 20-mW diode laser (Coherent, Santa Clara, CA), a GFP filter, a CSU21 confocal scanning system (Yokogawa Electronics, Tokyo, Japan), an AP imager camera (Hamamatsu Photonics, Hamamatsu, Japan), and an image intensifier unit (Hamamatsu Photonics). Images were analyzed with IPlab software (Scanalytics, Fairfax, VA).

Culture conditions for microscopy. For observations of cover glass cultures, approximately 10^3 conidia were inoculated in 100 μl of CD on coverslips that were placed in sealed petri dishes and incubated for 20 h at 30°C.

For observations with the inverted confocal microscope, approximately 10^3 conidia were inoculated in 100 μl of CD in a 35-mm glass base dish (Asahi Techno Glass, Chiba, Japan), which is a small petri dish whose bottom was made with cover glass, and incubated for 18 to 72 h at 30°C.

Observations of aerial and glass surface hyphae (see Results for definition) were performed essentially as described by Ishi et al. (15) with slight adaptations. In brief, approximately 1-mm-thick CD containing 2% agar was excised as a square of 1 cm by 1 cm and placed on a glass slide. Conidia were inoculated on the side surface of the CD agar medium, and hyphae were allowed to grow in lateral directions by preventing upward-directed growth with a cover glass. The culture was incubated at 30°C for up to 4 days in a petri dish containing a wet paper towel to prevent drying.

For observation of vacuoles in germinating conidia, fresh conidia collected from 5- to 6-day cultures in a CD plate were suspended in DPY at a concentration of 10^7/ml. The cultures were incubated at 30°C with shaking for ~6 h.

Staining of vacuoles. FM4-64 staining was performed as follows. Cultivation media of coverslip cultures were replaced with CD containing 8 μM FM4-64, and the cultures were incubated for 10 min at 30°C. The media containing the dye were replaced twice with fresh media without dye, and the cultures were incubated at 30°C for another 10 min, followed by microscopy observations. CMAC staining of vacuoles was performed as described previously (23). Dual staining with FM4-64 and CMAC was carried out as follows. Cover glass cultures were first incubated in CD containing 10 μM CMAC for 15 min, followed by incubation for another 15 min in CD containing both 10 μM CMAC and 8 μM FM4-64. After being washed with fresh dye-free medium, the cover glass cultures were observed.

CFDA staining of yeast vacuoles was performed as described by Roberts et al. (28).

Measurement of apical extension rate. Conidia of RIB40, the *A. oryzae* wild-type strain, were inoculated in 100 μl of CD in glass base dishes and incubated for 20 h at 30°C. The culture media were then replaced with either CD (control) or CD containing 8 μM FM4-64 and incubated for 30 min. The culture dishes were then placed on a Thermo Plate (Tokai Hit Co., Shizuoka, Japan) set at 30°C and observed with a 40× objective lens. Hyphae at the mycelial periphery were selected for measurement, since other hyphae lying in the growth direction might have influenced hyphal growth. Two pictures that were taken at intervals of 10 min were overlaid, and the distance between the respective hyphal tips was defined as the hyphal elongation length per 10 min.

RESULTS

Cloning and characterization of Ao*vam3*, the *VAM3* homologue gene in *A. oryzae*. The cDNA of the *S. cerevisiae VAM3* homologue gene in *A. oryzae* was cloned using a PCR-based approach. To obtain the genomic DNA of the gene, plaque hybridization for *A. oryzae* genomic DNA library (13) was performed essentially as described previously (21). Sequence analysis revealed that the gene contains a single intron and encodes a putative protein product of 271 amino acids (DDBJ nucleotide sequence database accession no. AB232045). This gene was designated Ao*vam3*, since this is the only gene in the *A. oryzae* genome database (20) that encodes a putative protein displaying high sequence identity to *S. cerevisiae* Vam3p (25.2%). In addition, AoVam3p has characteristic features of the syntaxin family t-SNAREs, such as a SNARE motif and a predicted transmembrane domain at the carboxy terminus. Notably, the AoVam3p sequence also showed an equal level of identity to *S. cerevisiae* Pep12p (27.1%), a t-SNARE in the late endosome/prevacuolar compartment (3). Thus, as was predicted in other filamentous fungi (12), *A. oryzae* possesses only one gene corresponding to either *VAM3* or *PEP12*.

As Ao*vam3* showed sequence similarity to both *VAM3* and *PEP12*, we were interested in determining whether Ao*vam3*

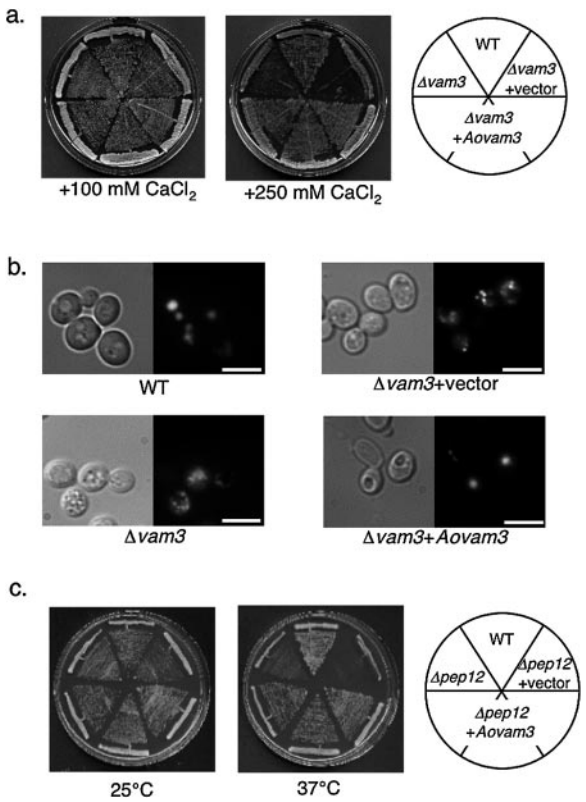

FIG. 1. Complementation of *S. cerevisiae* Δ*vam3* and Δ*pep12* phenotypes by the expression of Ao*vam3* cDNA. (a) The indicated yeast strains were streaked on the YPGal plate containing either 100 mM or 250 mM $CaCl_2$ and grown for 3 days. (b) Vacuoles of the indicated strains were stained with 10 μM CFDA. Large developed vacuoles were observed in the wild-type (WT) strain and the Δ*vam3* strain that expressed Ao*vam3* cDNA, while Δ*vam3* strain that only possessed the empty vector showed vacuolar fragmentation. Bars, 10 μm. (c) The indicated yeast strains were streaked on the YPGal plate and incubated at either 25°C or 37°C for 3 days.

was also functionally homologous to these genes. To test this, we performed complementation analyses for *S. cerevisiae* deletion mutants. Deletion of *VAM3* causes a growth defect in the presence of a high concentration of calcium (36). As shown in Fig. 1a, however, expression of the Ao*vam3* cDNA restored the growth in the presence of 250 mM $CaCl_2$ (Fig. 1a). Vacuolar fragmentation of the Δ*vam3* strain (44) was also complemented by the expression of the Ao*vam3* cDNA (Fig. 1b). On the other hand, deletion of *PEP12* causes a temperature sensitivity (3) and defects in maturation of vacuolar hydrolytic enzymes (8). We therefore tested the complementation of the CPY activity (data not shown) by APE assay (16) and the growth at 37°C (Fig. 1c). In both cases, the expression of the Ao*vam3* cDNA restored the defects in the Δ*pep12* mutant. These results indicate that AoVam3p is likely the vacuolar and/or endosomal t-SNARE in *A. oryzae*.

Generation of EGFP-AoVam3p-expressing strains. For the expression of AoVam3p fused at its amino terminus with EGFP (EGFP-AoVam3p) in *A. oryzae*, three strains, UEV1, TPVEV1, and TPVEV4, were generated (Table 1). In all three strains, EGFP was fused at the amino terminus of AoVam3p and therefore should locate on the cytosolic side. UEV1 carries the plasmid pUEGFP-VAM and overexpresses EGFP-AoVam3p under the strong, inducible promoter of *amyB* gene that encodes an α-amylase (37). UEV1 displayed no distinguishable differences in morphology compared with the control strain in glucose medium (data not shown) in which the *amyB* promoter was induced at the intermediate level (37), suggesting that overexpression of EGFP-AoVam3p does not impair the integrity of the mycelium. In some cases, however, overexpression and fusion of a t-SNARE with EGFP result in mislocalization or leakage of the fusion protein to other organelles (4). We therefore tested whether the expression of EGFP-AoVam3p can complement the phenotypes of the Ao*vam3* conditional expression strain (J.-Y. Shoji, M. Arioka, and K. Kitamoto, unpublished results) to determine whether the fusion protein is functional. The TPVII118 strain, an Ao*vam3* conditional expression strain, expresses Ao*vam3* under the thiamine-regulatable *thiA* promoter (35) and is defective in aerial hyphal formation, so that its mycelium shows a rough periphery in the Ao*vam3*-repressed condition. These phenotypes were complemented in TPVEV strains that expressed EGFP-AoVam3p under the control of the Ao*vam3* promoter on a TPVII118 background (Fig. 2). This observation confirmed that the fusion protein is functional. Southern analysis of TPVEV1, 2, 3, and 4 revealed that single copies of the plasmid were inserted homologously at the *niaD* locus in the TPVEV1, 2, and 3 strains, while a few extra copies of the plasmid (probably one or two additional copies, judged by the signal intensity) had been inserted in the TPVEV4 strain (data not shown). Therefore, the expression level of EGFP-AoVam3p is similar to that of authentic AoVam3p in TPVEV1, while the

TABLE 1. Genotypes of strains used in this study

Name	Parental strain	Genotype	Expression level of EGFP-AoVam3p
RIB40		Wild type	
niaD300	RIB40	*niaD*$^-$	
NS4	niaD300	*niaD*$^-$ *sC*$^-$	
TPVII118[a]	NS4	*niaD*$^-$ *sC*$^-$ ΔAovam3::(*PthiA*-Ao*vam3 sC*)	
UEV1	niaD300	*niaD*$^-$::(*PamyB-egfp*-Ao*vam3 niaD*)	Overexpressed
TPVEV1	TPVII118	*niaD*$^-$::(*PAovam3-egfp*-Ao*vam3 niaD*) *sC*$^-$ ΔAovam3::(*PthiA*-Ao*vam3 sC*)	Similar to that of the authentic Aovam3
TPVEV4	TPVII118	*niaD*$^-$::(*PAovam3-egfp*-Ao*vam3 niaD*) *sC*$^-$ ΔAovam3::(*PthiA*-Ao*vam3 sC*)	Slightly overexpressed

[a] TPVII118 is an Ao*vam3* conditional expression mutant in which the entire Ao*vam3* coding sequence is replaced by *A. nidulans sC* and *A. oryzae thiA* promoter followed by Ao*vam3* cDNA.

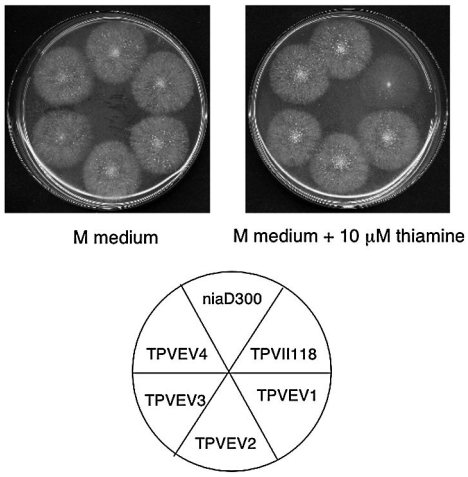

FIG. 2. Complementation of phenotypes in an Ao*vam3* conditional expression mutant by the expression of EGFP-AoVam3p. Approximately 10^2 conidia of either TPVII118, an Ao*vam3* conditional expression mutant that expresses Ao*vam3* under the control of thiamine-regulatable *thiA* promoter, and TPVEV strains that express EGFP-AoVam3p under the Ao*vam3* promoter on a TPVII118 background were inoculated and grown for 4 days in M medium (*thiA* promoter induced, left) or M medium containing 10 μM thiamine (*thiA* promoter repressed, right).

fusion protein is slightly overexpressed in TPVEV4 and is evidently overexpressed in UEV1.

EGFP-AoVam3p localized on the vacuolar membrane. In all three strains, EGFP-AoVam3p localized on small punctate structures in the apical region (Fig. 3b and e) and on tubular vacuoles in more distal compartments (Fig. 4). In the basal region of hyphae (Fig. 3a, c, d, f, and g), the membrane of large developed vacuoles and a few small punctate structures were observed with EGFP-AoVam3p (Fig. 3f and g). As the localization pattern of EGFP-AoVam3p was fundamentally similar in these strains (Fig. 3a to d and data not shown), we present the representative results of one of these transformants in the following studies, although essentially similar results were obtained for all three strains tested.

We next performed FM4-64 and CMAC staining of UEV1, TPVEV1, and TPVEV4 to compare the staining patterns of the dyes with EGFP fluorescence. In *S. cerevisiae*, FM4-64 stains endosomal compartments such as endosomes and vacuoles (43). In filamentous fungi, some arguments remain on its means of internalization and possible cytotoxic effects (6, 40). FM4-64 is believed to be internalized by endocytosis and accumulates in endosomal organelles (10). CMAC permeates into the cytoplasm due to its hydrophobic character and is converted to a cell-impermeant conjugate with glutathione by glutathione *S*-transferase. In fungi, CMAC accumulates in vacuoles, presumably via the action of glutathione pumps on the vacuolar membrane.

As some reports pointed out possible toxic effects of FM4-64 and subsequent artifactual results (6, 40), we first investigated the effects of the dye on *A. oryzae* cultures. The growth rates of hyphal tips in CD medium in the presence of 8 μM FM4-64 (1.01 ± 0.16 μm min^{-1}, $n = 8$) were similar to those in the absence of FM4-64 (0.98 ± 0.19 μm min^{-1}, $n = 8$). Vacuolar morphology judged by EGFP-AoVam3p was not affected by the presence of FM4-64 (Fig. 3). We also carried out dual staining of cover glass cultures with FM4-64 and CMAC. In the mycorrhizal fungus *P. tinctorius*, FM4-64 showed good labeling of vacuolar membranes in only dead or damaged hyphae and was scarcely observed on the membrane of intact vacuoles that accumulated CMAC (6). However, this was not the case in *A. oryzae*, and the membranes of most CMAC-positive vacuoles were stained by FM4-64 (Fig. 3g). From these results, we concluded that FM4-64 did not affect mycelial physiology in *A. oryzae* under our experimental conditions.

FM4-64 and EGFP-AoVam3p colocalized on the membrane of large developed vacuoles as well as on small punctate structures throughout hyphae (Fig. 3a to d). In extreme apices, where FM4-64 showed a diffuse and uneven staining pattern, however, EGFP fluorescence was normally absent (Fig. 3b). The diffuse and uneven fluorescence of FM4-64 seems to correspond to putative endosomes and a cloud of stained endocytic vesicles that are most rapidly stained by FM4-64 (10). In conclusion, EGFP-AoVam3p localizes in endocytic compartments, vacuoles, and possibly endosomes, but is likely absent in the early endocytic compartments.

The staining pattern of CMAC also showed good coincidence with EGFP-AoVam3p (Fig. 3e and f). The membrane of vacuoles that were stained by CMAC was always visualized by EGFP-AoVam3p (Fig. 3e and f). However, there were some small punctate structures visualized by EGFP-AoVam3p, often positioned adjacent to large vacuoles, that showed no or only faint staining by CMAC (Fig. 3f and g). As FM4-64 also stained them (Fig. 3g), these punctate structures are endocytic compartments. These observations led us to speculate that these structures are late endosomes/prevacuolar compartments, since they have common properties with the class E compartments, enlarged late endosomes/prevacuolar compartments in yeast class E *vps* mutants (27), in that they can be visualized by a vacuolar membrane protein and endocytic tracers and that they reside next to vacuoles. Overall, EGFP-AoVam3p localizes on the membrane of large and small vacuoles stained by both FM4-64 and CMAC. In addition, the fusion protein also localized on the putative late endosomes/prevacuolar compartments that were stained by FM4-64 but not by CMAC.

Confocal microscopy of EGFP-AoVam3p-expressing strains. To further study the vacuolar morphology in *A. oryzae*, we performed confocal microscopy on EGFP-AoVam3p-expressing strains grown in glass base dishes. The use of glass base dishes allowed a longer incubation period than the use of cover glass cultures, and cultures grown for up to 72 h were observed. Time-lapse imaging of EGFP-AoVam3p revealed the dynamics of pleomorphic vacuolar networks in *A. oryzae* (Fig. 4a to c; see image series in the supplemental material). Even the large developed vacuoles that seemed to be rather stable over a short time period changed in number, size, and position in minutes, most probably reflecting fusion and fission of vacuoles (Fig. 4a; see series A in the supplemental material). In basal hyphae, where many vacuoles formed clusters, small vesicle-like structures occasionally moved between large vacuoles (Fig. 4b). A tubular vacuole was then formed from a small punctate structure (Fig. 4b) and replaced the vesicle-like structures to interconnect the spherical vacuoles directly (Fig. 4b; see series B in the supplemental material). In the subapical region, where

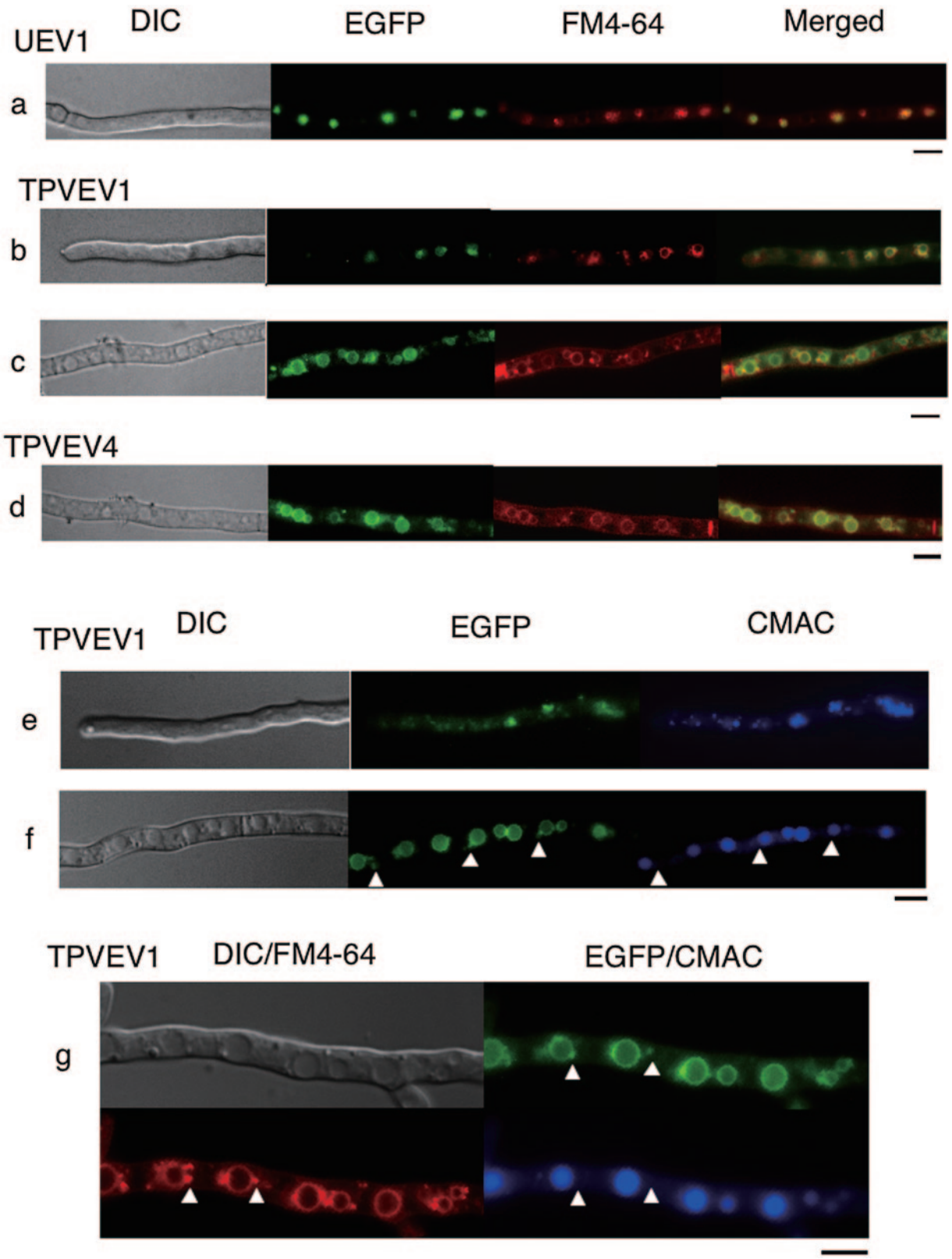

FIG. 3. FM4-64 and CMAC staining of EGFP-AoVam3p-expressing strains. Cover glass cultures of UEV1, TPVEV1, and TPVEV4 grown for 20 h at 30°C were stained with either 8 μM FM4-64 (a to d) or 10 μM CMAC (e, f). (a) Basal region in UEV1. (b, c) Apical region and basal region, respectively, in TPVEV1. (d) Basal region in TPVEV4. (e, f) Apical and basal regions, respectively, in TPVEV1. (g) Dual staining of TPVEV1 with FM4-64 and CMAC. Images of DIC, FM4-64, EGFP, and CMAC fluorescence are shown. Arrowheads (f, g) indicate putative late endosomes/prevacuolar compartments visualized by EGFP-AoVam3p that are not stained with CMAC. Bars, 5 μm.

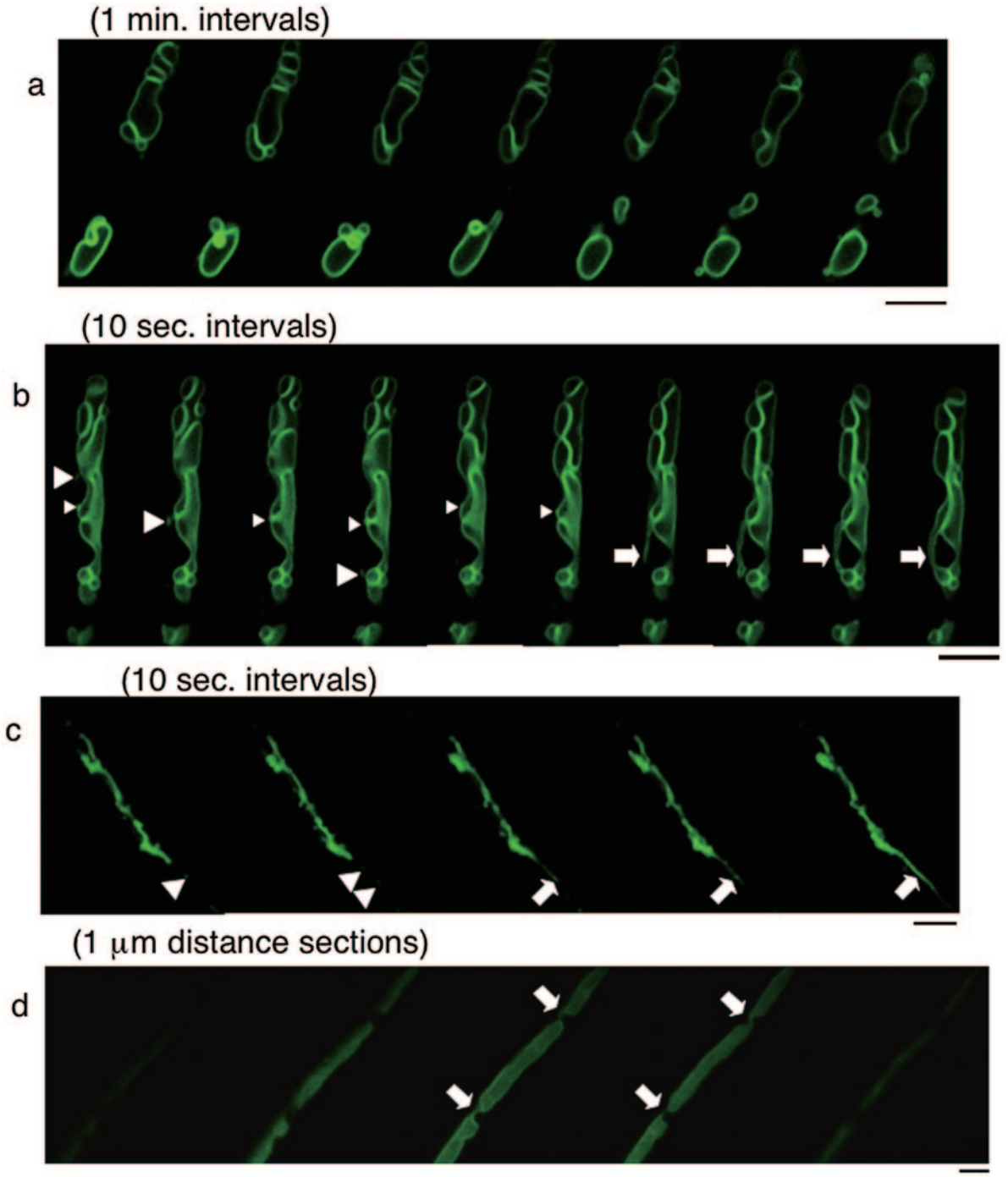

FIG. 4. Confocal microscopy of EGFP-AoVam3p-expressing strains. UEV1 was grown in glass base dishes for 20 h (a to c) or 48 h (d) and observed with inverted confocal laser scanning microscopy. (a) Time-lapse images of large vacuoles taken at intervals of 1 min. Vacuoles changed in size, position, and number over time. (b) Time-lapse images of vacuoles taken at intervals of 10 s. Moving punctate structures (large arrowheads), putative late endosomes/prevacuolar compartments (small arrowheads), and tubular vacuoles (arrows) that replaced the punctate structures are shown. (c) Time-lapse images of a tubular-vesicular cluster taken at intervals of 10 s. Moving punctate structures (arrowheads) and a tubular vacuole (arrows) that replaced the punctate structures were also observed here. (d) Distance sections (1 μm) of vacuoles in the basal region. The entire lumen was occupied with EGFP fluorescence. Tubular vacuoles (arrows) interconnected these vacuoles. Bars, 5 μm.

clusters of small punctate structures and tubular vacuoles formed a continuum, reversible transformations between the punctate structures and tubular vacuoles were often observed. (Fig. 4c; see series C in the supplemental material).

Observation with confocal microscopy highlighted the localization of EGFP-AoVam3p on the membrane (Fig. 4a and b). In old hyphae that were often observed in 2-day cultures in glass base dishes, however, membrane localization of the fu-

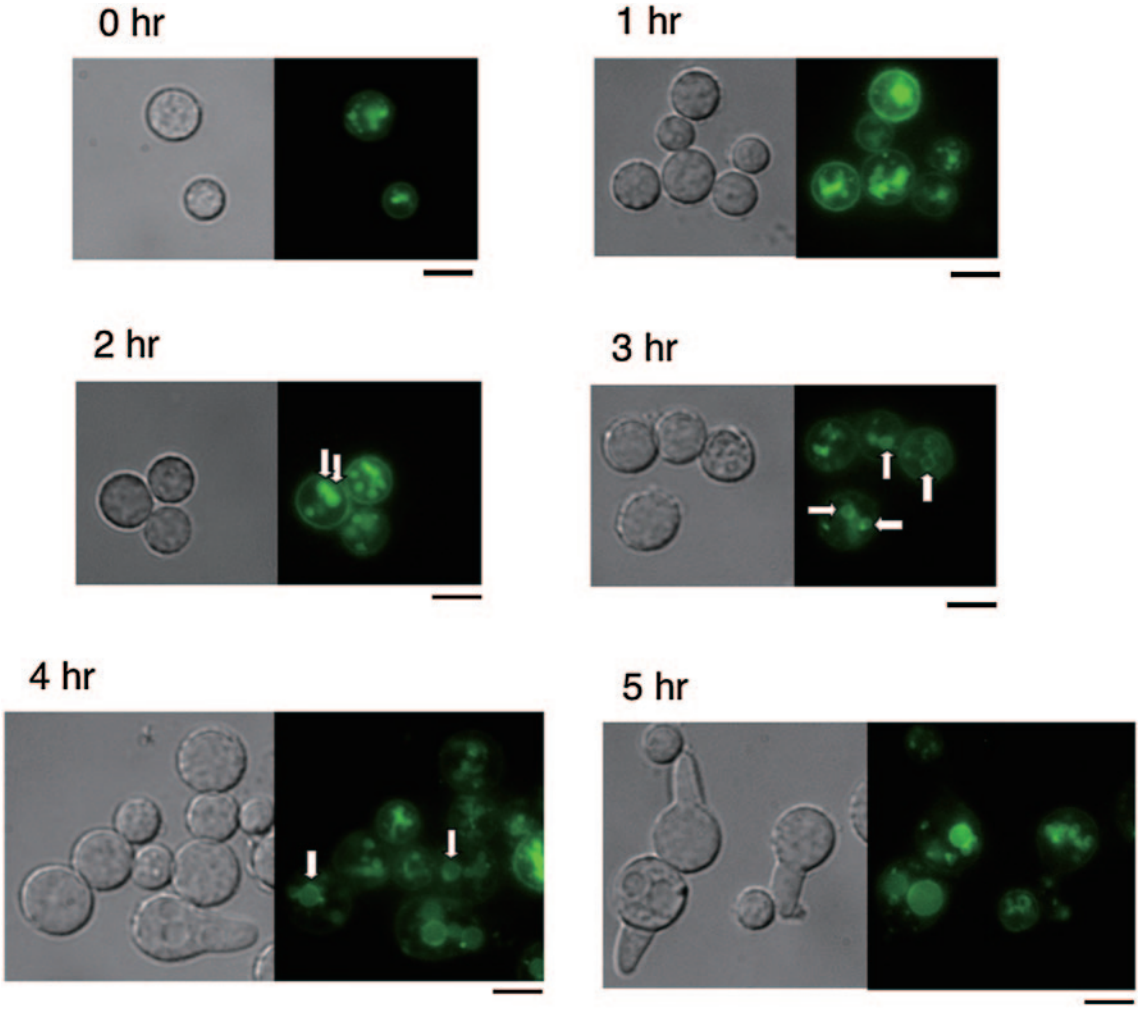

FIG. 5. Vacuolar morphology in germinating conidia. DIC images (left) and EGFP fluorescence (right) of conidia from TPVEV1 at the time indicated after inoculation into DPY medium. Large vacuoles (>1 μm) that eventually developed in swelling conidia approximately 2 h after inoculation are indicated by arrows. Fluorescence at the cell periphery was also detected in a control strain that did not express EGFP and was therefore judged as autofluorescence. Bars, 5 μm.

sion protein was not clear (Fig. 4d). In all sections of 1-μm distance taken with a confocal microscope, EGFP fluorescence was observed throughout the vacuolar lumen and was not restricted to the membrane. Such topological changes in EGFP fluorescence localization should require budding of the vacuolar membrane into the lumen. Since vacuoles often occupied the greater part of cells in these hyphae (Fig. 4d), internalization of EGFP-AoVam3p into the vacuolar lumen is likely achieved via an autophagic process (19). Interestingly, these vacuoles were often interconnected by tubular vacuoles (Fig. 4d).

Vacuoles in various developmental stages. We next observed vacuoles in several developmental stages, conidial germination, and aerial hyphae. In conidia just after inoculation (Fig. 5, 0 h), small punctate vacuoles (<1 μm) and clouds of fluorescence were observed with EGFP-AoVam3p. At 2 h after inoculation, larger vacuoles (>1 μm) eventually emerged (Fig. 5), concomitant with conidial swelling. Vacuoles enlarged further, and at 3 to 4 h after inoculation, large spherical vacuoles (2 to 5 μm) appeared in swollen or germinating conidia (Fig. 5), accompanied by a few small punctate structures. In germ tubes, large vacuoles were normally absent and small punctate structures were often observed.

We next observed hyphae that were not in contact with nutrients. Conidia were inoculated on the side surface of approximately 1-mm-thick CD agar, and hyphae were allowed to grow in lateral directions by preventing upward-directed growth with a cover glass. Under these conditions, three kinds of hyphae that grew laterally were observed, hyphae that grew in/on the agar medium and two kinds of hyphae that were not in contact with nutrients, hyphae that grew in the air (aerial hyphae) and hyphae that grew on the cover glass surface (glass surface hyphae). These hyphae almost always had yellowish fluorescence at the cell wall or plasma membrane and at hyphal tips, even in the wild-type strain that does not express EGFP (Fig. 6j and k, respectively). Based on this observation, fluorescence at the cell periphery in Fig. 6 was considered to be autofluorescence. In the wild-type strain, green organelle-like

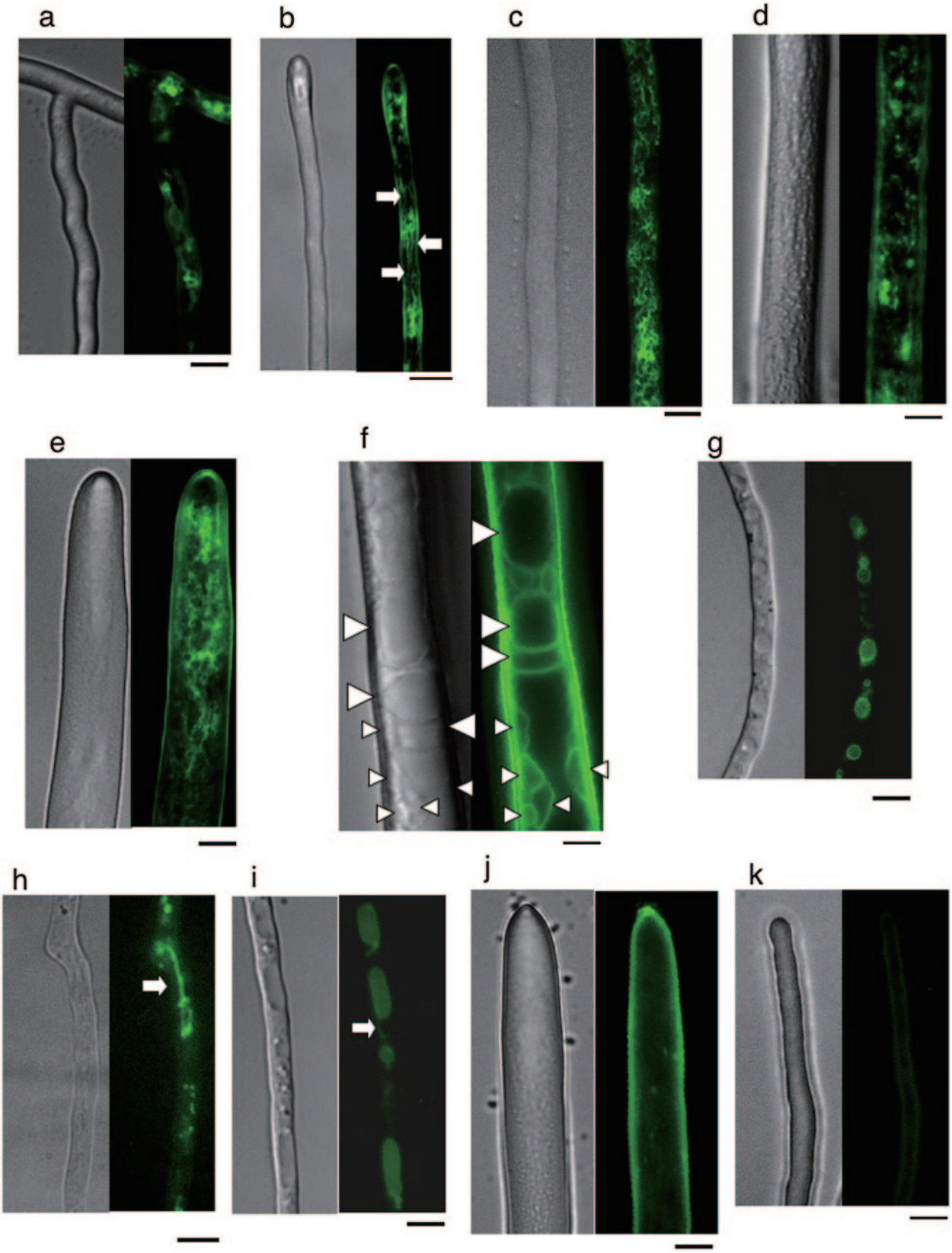

FIG. 6. Vacuolar morphologies in hyphae that are not in contact with nutrients. Conidia of TPVEV4 were inoculated on the side of approximately 1-mm-thick CD containing 2% agar, and hyphae were allowed to grow in lateral directions for 48 h (a to e, g, h) or 72 h (f, i) by preventing the upward-directed growth with a cover glass. Pictures of the glass surface hyphae and the aerial hyphae were prepared under the respective identical conditions of exposure time and contrast enhancement. In all figures, fluorescence at the cell wall/membrane is judged as

fluorescence inside cells, such as that shown in Fig. 6a to i, was never observed (Fig. 6j and k). In glass surface hyphae that were judged by their thickness of <4 μm, large vacuoles (>2 μm) were rather rare and were restricted to the region near the agar medium, where liquid enclosed the hyphae. Instead, small vacuoles (500 nm to 1 μm in diameter) were predominant (Fig. 6a to c). In addition, tubular vacuoles interconnecting the small vacuoles were more often observed in the glass surface hyphae (Fig. 6b) than in hyphae that were in contact with nutrients. Such tubular-vesicular clusters were sometimes so dense that they showed a rather reticulum-like appearance (Fig. 6c).

In aerial hyphae that were distinguished from glass surface hyphae by their thickness of >5 μm, vacuoles were present as small punctate structures (Fig. 6d). Tubular vacuoles that extended in the longitudinal direction and had a reticular appearance were also observed in aerial hyphae (Fig. 6e) but at a lower frequency than glass surface hyphae. There were also aerial hyphae that had entirely strong yellowish autofluorescence and no greenish EGFP fluorescence, suggesting that some aerial hyphae had begun to die in the 2-day cultures. Interestingly, large vacuoles were present in aerial hyphae in 3- to 4-day cultures (Fig. 6f). Some of these vacuoles flew (approximately 5 μm s^{-1}) toward the hyphal tips (Fig. 6f), but others positioned near the plasma membrane remained immobile (Fig. 6f, compare with the differential interference contrast [DIC] image that was taken several seconds later). As these hyphae were often enclosed in liquid droplets, the physical condition of such hyphae may differ from that of authentic aerial hyphae. In hyphae in/on the agar medium, in contrast, the vacuolar morphology was identical to that observed in cover glass and glass base dish cultures. Large developed vacuoles (Fig. 6g) and tubular vacuoles (Fig. 6 h), vacuoles whose lumen was occupied with EGFP fluorescence and were interconnected with tubular vacuoles (Fig. 6i), were observed. In conclusion, vacuoles showed characteristic morphology in hyphae that were not in contact with nutrients, with vacuoles forming highly reticular networks composed of tubular vacuoles, and with small punctate vacuoles.

DISCUSSION

Thus far, studies on vacuoles in filamentous fungi have made great progress in highlighting vacuolar morphology using fluorescence and electron microscopy. These studies identified the presence of highly pleomorphic dynamic vacuoles, such as tubular vacuoles, in filamentous fungi (reviewed in reference 2). In this report, we established three strains expressing the fusion protein of EGFP with AoVam3p, a putative vacuolar t-SNARE in *Aspergillus oryzae*. In contrast to conventional methods, in which the vacuolar lumen is stained with either CFDA derivatives (2, 6, 7, 34, 42) or CPY-EGFP (23, 24), EGFP-AoVam3p visualizes vacuolar membranes and therefore allowed us to observe vacuolar membrane dynamics at high resolution easily and reproducibly. Furthermore, several aspects of fungal vacuoles that had not been paid much attention previously, such as vacuoles in aerial and glass surface hyphae, as well as the internalization of EGFP fluorescence in the vacuolar lumen in old hyphae, were demonstrated for the first time using our observation system.

Does AoVam3p localize and act as a t-SNARE on both vacuoles and late endosomes/prevacuolar compartments? As Ao*vam3* is the only obvious homologue of yeast *VAM3* and *PEP12* in *A. oryzae*, it is possible that AoVam3p acts as the t-SNARE on both the vacuoles and the late endosomes/prevacuolar compartments. In our yeast complementation analysis, Ao*vam3* was capable of compensating the functions of both *VAM3* and *PEP12*, suggesting that AoVam3p is most likely the vacuolar and/or endosomal t-SNARE in *A. oryzae*. We cannot yet conclude, however, that AoVam3p plays the roles of both Vam3p and Pep12p in *A. oryzae*, since in *S. cerevisiae*, overexpression of Vam3p complements a *pep12* null mutant and, at least in part, vice versa (11). Moreover, Vam3p can complement a *pep12* null mutant even not overexpressed when its dileucine sorting signal is mutated (9). The dileucine sorting signal of Vam3p is required for its delivery from the Golgi apparatus to the vacuole via the alkaline phosphatase pathway that bypasses the late endosome/prevacuolar compartment. Mutations in the dileucine signal lead to missorting of Vam3p to the CPY pathway, the delivery route from the Golgi apparatus to the vacuole via the late endosome/prevacuolar compartment, and Vam3p that partially localizes on the late endosome/prevacuolar compartment compensates for the function of Pep12p (9). These results imply that if a Vam3p/Pep12p homologue can localize on both the vacuole and the late endosome/prevacuolar compartment, it can compensate for the roles of both Vam3p and Pep12p. Therefore, it was of importance to determine the localization of AoVam3p in *A. oryzae*. As revealed by FM4-64 and CMAC staining, EGFP-AoVam3p localized on CMAC-negative, nonvacuolar structures in addition to vacuoles. These CMAC-negative structures resembled class E *vps* compartments, enlarged late endosomes/prevacuolar compartments in yeast class E *vps* mutants (27), in that they can be visualized with vacuolar membrane proteins, they are adjacent to vacuoles, and they are endocytic compartments. Taken together, it is apparent that EGFP-AoVam3p localizes on late endosomes/prevacuolar compartments in addition to vacuoles. Exploration for possible candidates of late endosome/prevacuolar compartment-resident proteins will be

autofluorescence (see text). (a to c) Glass surface hyphae; (d to f) aerial hyphae; (g to i) hyphae in/on the agar medium. (a) Small vacuoles that are predominant in a glass surface hypha. (b) Clusters of small vacuoles interconnected with tubular vacuoles (arrows). (c) Tubular-vesicular vacuoles with a reticulum-like appearance. (d) Punctate vacuoles in an aerial hypha. (e) Tubular-reticular networks in an aerial hypha. (f) Large vacuoles in an aerial hypha that were observed in 3-day cultures. Some of these vacuoles moved toward the hyphal tips (large arrowheads), while others remained immobile (small arrowheads). (g) Large vacuoles in the agar medium. (h) A tubular vacuole in agar medium. (i) Vacuoles that are interconnected with tubular vacuoles in the basal region. The lumen of these vacuoles was entirely occupied with EGFP fluorescence. (j) Autofluorescence in a glass surface hypha of RIB40 strain that does not express EGFP-AoVam3p. (k) Autofluorescence in an aerial hypha of RIB40. As the pictures were taken with a monochromic camera and subsequently pseudocolored, yellowish autofluorescence appears green on this figure. Bars, 5 μm.

necessary for the further identification of late endosomes/prevacuolar compartments in filamentous fungi.

Enlargement of vacuoles in germinating conidia. Besides their roles in hyphal growth, fungal vacuoles may also be important in several developmental stages. Consistent with this, our observation demonstrated that swelling of conidia was accompanied by vacuolar enlargement. Moreover, in germinating conidia of *Colletotrichum graminicola*, lipid droplets are taken up and degraded by vacuoles (31), accompanied by vacuolar expansion (32). Further investigations of possible roles of vacuoles (e.g., storage degradation and cell expansion) may help us to understand the mechanism of conidial germination in filamentous fungi.

What is the role of tubular vacuoles in *A. oryzae*? Motile tubular vacuoles were first discovered in the mycorrhizal fungus *P. tinctorius* by electron microscopy and CFDA staining (34), and it has been proposed that they are endosomal compartments involved in intra- and intercellular transport (for a detailed discussion, see reference 2). We observed that a tubular vacuole was formed from small punctate structures and replaced vesicle-like structures. This result is consistent with the previous report on CFDA staining of vacuoles (34) and supports the notion that tubular vacuoles transport materials such as nutrients. In mycorrhizal fungi, there is an urgent need for bidirectional transport of nutrients; phosphorus and nitrogen compounds must be transported from hyphal tips to the plant interface, while carbon compounds that are supplied by plants should move to hyphal tips, where metabolic activity is the highest (2). Consistent with this hypothesis, tubular vacuoles of *P. tinctorius* contain phosphorus compounds (6). Given that tubular vacuoles are transport compartments, then why do they also exist in other filamentous fungi that do not have such a dependency on nutrients from other organisms? We found that tubular vacuoles interconnected large vacuoles in old hyphae that were often evident in 2- to 3-day cultures. As these vacuoles occupied the greater part of compartments and included EGFP fluorescence in the entire lumen, autophagic degradation of cytosolic materials and subsequent internalization of the vacuolar membrane into the lumen had possibly occurred in such compartments. An attractive explanation for a role of these tubular vacuoles is that they transport the degraded materials in old hyphae to more fresh and active regions in the mycelium. We also discovered that tubular vacuoles and clusters of small punctate vacuoles were prominent in hyphae that were not in contact with nutrients, especially in glass surface hyphae. Since these hyphae should have a more urgent requirement for nutrient transport, it is reasonable to speculate that tubular vacuoles develop more extensively in these hyphae and mediate transport of nutrients from hyphae that are in contact with media.

To date, nothing is known about the molecular machinery involved in the formation of tubular vacuoles, except the possible involvement of certain dynamin-like GTPases for tubule formation (14). AoVam3p is the first protein to be discovered that locates on the membrane of tubular vacuoles. As AoVam3p is a putative vacuolar t-SNARE that may mediate the heterotypic and homotypic fusion of vacuoles, it is quite possible that AoVam3p has important roles in regulating fungal pleomorphic vacuolar networks: fusion of small moving structures and tubular vacuoles with spherical vacuoles may be mediated by AoVam3p. The functional analysis of AoVam3p and its possible interacting partners will lead to better understanding of the precise mechanisms and roles of vacuolar networks in filamentous fungi.

Aerial hyphae of filamentous fungi. Although filamentous fungi can grow in liquid and on solid substrates, they are perhaps best known for their fuzzy aerial appearance. However, studies on these aerial structures have so far mainly focused on conidiation (see reference 1 for a review), and the specific phenomenon of aerial hyphae is only known for hydrophobins (38). To the best of our knowledge, our research is the first report on the observation of an organelle in the aerial hyphae of filamentous fungi. As our data demonstrated, the vacuolar morphology in aerial hyphae visualized by EGFP-AoVam3p was essentially different in appearance from that of hyphae in the medium. We assume that vacuolar morphology is characteristically regulated in aerial and glass surface hyphae to adapt to the unusual environment in terms of nutrients and osmotic pressure. As mentioned above, vacuoles showed a highly reticular-tubular appearance in aerial hyphae. As nutrients and/or materials for cell elongation should be delivered to aerial hyphae from basal compartments, vacuoles possibly mediate intra- and intercellular transport in these hyphae.

The characteristic vacuolar morphology is probably just an aspect of aerial hyphae, and other physical activities such as metabolism and morphogenesis are also differentially regulated in these hyphae. To date, essentially nothing is known about the molecular mechanisms regulating the metabolism and morphology of aerial hyphae, presumably because, at least in part, they are not well developed or clearly recognizable in *A. nidulans*, a model filamentous fungus. In *A. oryzae*, aerial hyphae grow approximately 5 mm in 2 days under our conditions and are therefore easily observed using microscopy. Further investigation of aerial hyphae in *A. oryzae* will compensate for the lack of this feature in *A. nidulans* and bring new insights to fungal physiology.

ACKNOWLEDGMENTS

This study was supported by a grant-in-aid for scientific research (B) (no. 15380058) to K.K. from the Ministry of Education, Culture, Sports, Science, and Technology, Japan, and a program for the promotion of basic research activities for innovative biosciences of the Bio-Oriented Technology Research Advancement Institution.

REFERENCES

1. **Adams, T. H., J. K. Wieser, and J. H. Yu.** 1998. Asexual sporulation in *Aspergillus nidulans*. Microbiol. Mol. Biol. Rev. **62:**35–54.
2. **Ashford, A. E.** 1998. Dynamic pleiomorphic vacuole systems: are they endosomes and transport compartments in fungal hyphae? Adv. Bot. Res. **28:** 119–159.
3. **Becherer, K. A., S. E. Rieder, S. D. Emr, and E. W. Jones.** 1996. Novel syntaxin homologue, Pep12p, required for the sorting of lumenal hydrolases to the lysosome-like vacuole in yeast. Mol. Biol. Cell **7:**579–594.
4. **Black, M. W., and H. R. Pelham.** 2000. A selective transport route from Golgi to late endosomes that requires the yeast GGA proteins. J. Cell Biol. **151**:587–600.
5. **Brachmann, C. B., A. Davies, G. J. Cost, E. Caputo, J. Li, P. Hieter, and J. D. Boeke.** 1998. Designer deletion strains derived from *Saccharomyces cerevisiae* S288C: a useful set of strains and plasmids for PCR-mediated gene disruption and other applications. Yeast **14:**115–132.
6. **Cole, L., D. A. Orlovich, and A. E. Ashford.** 1998. Structure, function, and motility of vacuoles in filamentous fungi. Fungal Genet. Biol. **24:**86–100.
7. **Cole, L., G. J. Hyde, and A. E. Ashford.** 1997. Uptake and compartmentalisation of fluorescent probes by *Pisolithus tinctorius* hyphae: evidence for an anion transport mechanism at the tonoplast but not for fluid-phase endocytosis. Protoplasma **199:**18–29.

8. **Cowles, C. R., W. B. Snyder, C. G. Burd, and S. D. Emr.** 1997. Novel Golgi to vacuole delivery pathway in yeast: identification of a sorting determinant and required transport component. EMBO J. **16:**2769–2782.
9. **Darsow, T., C. G. Burd, and S. D. Emr.** 1998. Acidic di-leucine motif essential for AP-3-dependent sorting and restriction of the functional specificity of the Vam3p vacuolar t-SNARE. J. Cell Biol. **142:**913–922.
10. **Fischer-Parton, S., R. M. Parton, P. C. Hickey, J. Dijksterhuis, H. A. Atkinson, and N. D. Read.** 2000. Confocal microscopy of FM4-64 as a tool for analysing endocytosis and vesicle trafficking in living fungal hyphae. J. Microsc. **198:**246–259.
11. **Götte, M., and D. Gallwitz.** 1997. High expression of the yeast syntaxin-related Vam3 protein suppresses the protein transport defects of a *pep12* null mutant. FEBS Lett. **411**:48–52.
12. **Gupta, G. D., and I. B. Heath.** 2002. Predicting the distribution, conservation, and functions of SNAREs and related proteins in fungi. Fungal Genet. Biol. **36**:1–21.
13. **Hirozumi, K., H. Nakajima, M. Machida, M. Yamaguchi, K. Takeo, and K. Kitamoto.** 1999. Cloning and characterization of a gene (*arpA*) from *Aspergillus oryzae* encoding an actin-related protein required for normal nuclear distribution and morphology of conidiophores. Mol. Gen. Genet. **262:** 758–767.
14. **Hyde, G. J., D. Davies, L. Cole, and A. E. Ashford.** 2002. Regulators of GTP-binding proteins cause morphological changes in the vacuoles system of the filamentous fungus, *Pisolithus tinctorius*. Cell Motil. Cytoskeleton **51:**133–146.
15. **Ishi, K., J. Maruyama, H. Nakajima, and K. Kitamoto.** 2005. Multinucleate conidia are not formed in conidia but through migration of plural nuclei from phialide in *Aspergillus oryzae.* Biosci. Biotechnol. Biochem. **69:**747–754.
16. **Jones, E. W.** 1977. Proteinase mutants of *Saccharomyces cerevisiae*. Genetics **85:**23–33.
17. **Kitamoto, K.** 2002. Molecular biology of the Koji molds. Adv. Appl. Microbiol. **51:**129–153.
18. **Klionsky, D. J., P. K. Herman, and S. D. Emr.** 1990. The fungal vacuole: composition, function, and biogenesis. Microbiol. Rev. **54:**266–292.
19. **Klionsky, D. J., and Y. Ohsumi.** 1999. Vacuolar import of proteins and organelles from the cytoplasm. Annu. Rev. Cell Dev. Biol. **15**:1–32.
20. **Kobayashi, T., K. Abe, K. Asai, K. Gomi, P. R. Juvvadi, M. Kato, K. Kitamoto, M. Takeuchi, and M. Machida.** Genomics of *Aspergillus oryzae.* Appl. Mycol. Biotechnol., in press.
21. **Kuroki, Y., P. R. Juvvadi, M. Arioka, H. Nakajima, and K. Kitamoto.** 2002. Cloning and characterization of *vmaA*, the gene encoding a 69-kDa catalytic subunit of the vacuolar H^+-ATPase during alkaline pH mediated growth of *Aspergillus oryzae*. FEMS Microbiol. Lett. **209:**277–282.
22. **Kutsuna, N., F. Kumagai, M. H. Sato, and S. Hasezawa.** 2003. Three-dimensional reconstruction of tubular structure of vacuolar membrane throughout mitosis in living tobacco cells. Plant Cell Physiol. **44:**1045–1054.
23. **Ohneda, M., M. Arioka, H. Nakajima, and K. Kitamoto.** 2002. Visualization of vacuoles in *Aspergillus oryzae* by expression of CPY-EGFP. Fungal Genet. Biol. **37:**29–38.
24. **Ohneda, M., M. Arioka, and K. Kitamoto.** 2005. Isolation and characterization of *Aspergillus oryzae* vacuolar protein sorting mutants. Appl. Environ. Microbiol. **71:**4856–4861.
25. **Ohsumi, K., M. Arioka, H. Nakajima, and K. Kitamoto.** 2002. Cloning and characterization of a gene (*avaA*) from *Aspergillus nidulans* encoding a small GTPase involved in vacuolar biogenesis. Gene **291:**77–84.
26. **Oka, M., J. Maruyama, M. Arioka, H. Nakajima, and K. Kitamoto.** 2004. Molecular cloning and functional characterization of *avaB*, a gene encoding Vam6p/Vps39p-like protein in *Aspergillus nidulans*. FEMS Microbiol. Lett. **232**:113–121.
27. **Raymond, C. K., I. Howald-Stevenson, C. A. Vater, and T. H. Stevens.** 1992. Morphological classification of the yeast vacuolar protein sorting mutants: evidence for a prevacuolar compartment in class E *vps* mutants. Mol. Biol. Cell **3:**1389–1402.
28. **Roberts, C. J., C. K. Raymond, C. T. Yamashiro, and T. H. Stevens.** 1991. Methods for studying the yeast vacuole. Methods Enzymol. **194:**644–661.
29. **Rothman, J. E.** 1994. Mechanisms of intracellular protein transport. Nature **372:**55–63.
30. **Sato, M. H., N. Nakamura, Y. Ohsumi, H. Kouchi, M. Kondo, I. Hara-Nishimura, M. Nishimura, and Y. Wada.** 1997. The *AtVAM3* encodes a syntaxin-related molecule implicated in the vacuolar assembly in *Arabidopsis thaliana*. J. Biol. Chem. **272:**24530–24535.
31. **Schadeck, R. J., B. Leite, and D. F. Buchi.** 1998. Lipid mobilization and acid phosphatase activity in lytic compartments during conidium dormancy and appressorium formation of *Colletotrichum graminicola*. Cell Struct. Funct. **23:**333–340.
32. **Schadeck, R. J., M. A. Randi, D. F. Buchi, and B. Leite.** 2003. Vacuolar system of ungerminated *Colletotrichum graminicola* conidia: convergence of autophagic and endocytic pathways. FEMS Microbiol. Lett. **218:**277–283.
33. Reference deleted.
34. **Shepherd, V. A., D. A. Orlovich, and A. E. Ashford.** 1993. A dynamic continuum of pleiomorphic tubules and vacuoles in growing hyphae of a fungus. J. Cell Sci. **104:**495–507.
35. **Shoji, J. Y., J. Maruyama, M. Arioka, and K. Kitamoto.** 2005. Development of *Aspergillus oryzae thiA* promoter as a tool for molecular biological studies. FEMS Microbiol. Lett. **244:**41–46.
36. **Srivastava, A., and E. W. Jones.** 1998. Pth1/Vam3p is the syntaxin homolog at the vacuolar membrane of Saccharomyces cerevisiae required for the delivery of vacuolar hydrolases. Genetics **148**:85–98.
37. **Tada, S., K. Gomi, K. Kitamoto, K. Takahashi, G. Tamura, and S. Hara.** 1991. Construction of a fusion gene comprising the Taka-amylase A promoter and the *Escherichia coli* beta-glucuronidase gene and analysis of its expression in *Aspergillus oryzae*. Mol. Gen. Genet. **229:**301–306.
38. **Talbot, N. J.** 1997. Growing into the air. Curr. Biol. **7:**78–81.
39. **Tarutani, Y., K. Ohsumi, M. Arioka, H. Nakajima, and K. Kitamoto.** 2001. Cloning and characterization of *Aspergillus nidulans vpsA* gene which is involved in vacuolar biogenesis. Gene **268:**23–30.
40. **Torralba, S., and I. B. Heath.** 2002. Analysis of three separate probes suggests the absence of endocytosis in *Neurospora crassa* hyphae. Fungal Genet. Biol. **37**:221–232.
41. **Uemura, T., S. H. Yoshimura, K. Takeyasu, and M. H. Sato.** 2002. Vacuolar membrane dynamics revealed by GFP-AtVam3 fusion protein. Genes Cells **7:**743–753.
42. **Uetake, Y., T. Kojima, T. Ezawa, and M. Saito.** 2002. Extensive tubular vacuole system in an arbuscular mycorrhizal fungus, *Gigaspora margarita*. New Phytol. **154:**761–768.
43. **Vida, T. A., and S. D. Emr.** 1995. A new vital stain for visualizing vacuolar membrane dynamics and endocytosis in yeast. J. Cell Biol. **128**:779–792.
44. **Wada, Y., N. Nakamura, Y. Ohsumi, and A. Hirata.** 1997. Vam3p, a new member of syntaxin related protein, is required for vacuolar assembly in the yeast *Saccharomyces cerevisiae*. J. Cell Sci. **110:**1299–1306.
45. **Wang, L., A. J. Merz, K. M. Collins, and W. Wickner.** 2003. Hierarchy of protein assembly at the vertex ring domain for yeast vacuole docking and fusion. J. Cell Biol. **160:**365–374.
46. **Wang, L., E. S. Seeley, W. Wickner, and A. J. Merz.** 2002. Vacuole fusion at a ring of vertex docking sites leaves membrane fragments within the organelle. Cell **108:**357–369.